Eur. Phys. J. C 1, 523–529 (1998)

THE EUROPEAN
PHYSICAL JOURNAL C

Radiatively corrected semileptonic spectra in B meson decays

Changhao Jin[1], Emmanuel A. Paschos[2]

[1] Sektion Physik, Universität München, Theresienstrasse 37, D-80333 München, Germany
(e-mail: jin@photon.hep.physik.uni-muenchen.de)
[2] Institut für Theoretische Physik, Universität Dortmund, D-44221 Dortmund, Germany

Received: 9 April 1997 / Revised version: 27 May 1997

Abstract. We show how radiative QCD corrections calculated in terms of quarks can be incorporated at the hadron level in inclusive semileptonic B-meson decays. The bound state effects are described by a momentum distribution function of the b quark. The summation over the final states and the averaging over the momentum distribution of the decaying quark render the radiative corrections finite. With this coherent formalism we investigate the shape of the electron spectra for $b \to u$ and $b \to c$ decays as a function of the parameters of the theory. The resultant $b \to c$ electron energy spectrum is in agreement with the experimental data.

1 Introduction

Semileptonic B-meson decays have been studied for some time now. The inclusive decays

$$\bar{B} \to X_q + e + \bar{\nu}_e \, , \tag{1}$$

with $\bar{B}$ representing B^- or $\bar{B}^0$ and X_q any possible hadronic final state containing a charm quark ($q = c$) or an up quark ($q = u$), provide information on both couplings V_{cb} and V_{ub}, as well as new information on the internal structure of the B-meson. In this paper we study the electron energy spectra. For the theoretical description of the electron spectra in (1), strong interactions in the underlying weak decays must be incorporated, since they are responsible for the confinement of quarks and gluons into hadrons. They will be included in two steps: as bound state effects and also in the form of gluons radiated during the decay.

For inclusive B-meson decays, it was recognized that extended regions of phase space involve large values of q^2, the momentum transfer squared, originating from the large mass of the B meson. Consequently the commutator of the two currents describing the decay is dominated by distances close to the light-cone. In this case it is justified to replace the commutator of the weak currents by their light-cone singularity times a bilocal operator in b-quark fields [1–3]. This replacement together with standard mathematical methods leads to general expressions of the decay spectra which involve a b-quark distribution function, whose origin is non-perturbative. Thus the semileptonic decays in (1) can be described, in direct analogy to deep inelastic scattering, in terms of a quark distribution function, which depends on a new scaling variable ξ_+.

It has also been recognized that the heavy quark field can be studied in an effective field theory derived from the QCD Lagrangian. The heavy quark effective theory (HQET) sets a framework for keeping track of the heavy quark mass dependence and for parametrizing nonperturbative phenomena. The effective theory has been successfully applied to inclusive B decays [4–12]. Using the operator product expansion and the method [5–7] of the HQET, it was possible to derive sum rules for the distribution function, which depend on the kinetic energy and the chromomagnetic energy of the b-quark in the B-meson. The numerical values for the sum rules are determined by static properties of B mesons and QCD sum rules [13]. The sum rules specify the mean value and the variance of the distribution function. They imply that the distribution function $f(\xi)$ peaks at large values of $\xi \approx 0.93$ and is very narrow.

In addition radiative QCD corrections must be included. The QCD radiative corrections to the electron energy spectra were computed [14–19] at the quark level. In the quark decay the phase space ends at the electron energy $E_e = \frac{m_b}{2}\left(1 - \frac{m_q^2}{m_b^2}\right)$, with m_b and m_q the masses of the b-quark and the final quark, respectively. The quark decay rates as well as the radiative corrections vanish for $E_e > \frac{m_b}{2}(1 - \frac{m_q^2}{m_b^2})$, whereas in reality the physical endpoint is $E_e = \frac{M}{2}(1 - \frac{M^2_{X_{min}}}{M^2})$ with M the mass of the B-meson and $M_{X_{min}}$ the minimum value of the invariant mass of the hadronic final state. In addition, the $O(\alpha_s)$ radiative corrections at the quark level have logarithmic singularities at the endpoints. For inclusive decays, however, we integrate over the phase space of the final quark and average over the momentum distribution of the initial quark in order to incorporate the bound state effect. These steps sum over ensembles of states, render the radiative corrections finite [20,21] and extend the phase space from the quark level to the hadron level.

In this way we have at our disposal a coherent treatment of perturbative and nonperturbative QCD effects. This treatment has the advantage of accounting correctly for the phase-space effects and producing the electron energy spectra which are smooth everywhere up to the physical endpoints. For instance, the spectrum is a smooth function of the electron energy E_e in the endpoint region between the $b \to c$ endpoint $E_e = \frac{M}{2}(1 - \frac{M_D^2}{M^2}) = 2.31$ GeV and the $b \to u$ endpoint $E_e = \frac{M}{2}(1 - \frac{M_\pi^2}{M^2}) = 2.64$ GeV, which is useful for extracting $|V_{ub}|$ since only the $b \to u$ transition is allowed in this region.

This paper contains a brief, but complete presentation of the various improvements of the parton model [1, 2] involved in the calculation of the semileptonic spectrum. For the sake of completeness we present in Sect. 2 the general formalism for inclusive semileptonic B meson decays. Then we show in Sect. 3 that the light-cone dominance provides a foundation for the parton model and a systematic framework for improving it by including QCD corrections. In these two sections, we point out how the general formula in (7) reduces to an expression for the decay rate in (24) in terms of a distribution function. The distribution function is constrained by three sum rules which are discussed in Sect. 4. Two of the sum rules were derived in the heavy quark effective theory and are now incorporated in the approach. One of our purposes is to calculate the electron energy spectra. For a meaningful calculation we must include QCD radiative corrections. In Sect. 5 we propose a method for including the QCD radiative corrections to bound states. The method is an improvement over the quark level results. It establishes that radiative corrections are finite and calculable (Fig. 1). All these improvements make possible, in Sect. 6, the calculations of the semileptonic spectra and the studies of their sensitivity to the underlying parameters. We find a satisfactory fit of the $b \to c$ spectrum for values of the parameters consistent with the sum rules (Fig. 7). The electron spectrum for $b \to u$ decays in the endpoint region 2.31 GeV$\leq E_e \leq$ 2.64 GeV is predicted and shown to be insensitive to two parametrizations of the distribution function (Fig. 4). This result should be useful for extracting $|V_{ub}|$.

2 General formalism

The inclusive semileptonic decays (1), in which the B meson of four-momentum P decays into an electron of four-momentum k_e and an antineutrino of four-momentum k_ν, are described by the decay amplitude

$$\mathcal{M} = V_{qb}\frac{G_F}{\sqrt{2}}\bar{u}(k_e)\gamma^\mu(1-\gamma_5)v(k_\nu)\langle n|j_\mu(0)|B\rangle\,. \qquad (2)$$

Here V_{qb} are the elements of the CKM matrix and $j_\mu(x)$ is the weak current, which in terms of quark fields is given by

$$j_\mu(x) = \bar{q}(x)\gamma_\mu(1-\gamma_5)b(x) \qquad (3)$$

and $|B\rangle$ is the B-meson state normalized according to $\langle B|B\rangle = 2P_0(2\pi)^3\delta^3(\mathbf{0})$. The basic quantity for the decay is the second rank tensor

$$W_{\mu\nu} = \sum_n \int \left[\prod_{i=1}^{n}\frac{d^3P_i}{(2\pi)^3 2E_i}\right](2\pi)^3\delta^4(P-q-\sum_{i=1}^{n}P_i)$$
$$\times\langle B|j_\nu^\dagger(0)|n\rangle\langle n|j_\mu(0)|B\rangle\,, \qquad (4)$$

where q stands for the four-momentum transferred from the decaying B meson to the lepton pair, $q = k_e + k_\nu$. It is useful to express the hadronic tensor in terms of a current commutator

$$W_{\mu\nu} = -\frac{1}{2\pi}\int d^4y e^{iq\cdot y}\langle B|[j_\mu(y), j_\nu^\dagger(0)]|B\rangle \qquad (5)$$

because the commutator is more convenient for theoretical considerations. The hadronic tensor can be decomposed in terms of scalars $W_a(q^2, q\cdot P)$, $a = 1,\ldots,5$, as follows:

$$W_{\mu\nu} = -g_{\mu\nu}W_1 + \frac{P_\mu P_\nu}{M^2}W_2 - i\varepsilon_{\mu\nu\alpha\beta}\frac{P^\alpha q^\beta}{M^2}W_3$$
$$+\frac{q_\mu q_\nu}{M^2}W_4 + \frac{P_\mu q_\nu + q_\mu P_\nu}{M^2}W_5\,. \qquad (6)$$

The tensor $(P_\mu q_\nu - q_\mu P_\nu)$ does not appear because of the time reversal invariance. We can express the differential decay rates in terms of the five hadronic structure functions W_a, $a = 1,\ldots,5$. The decay rate of the process (1) in the rest frame of the B meson is

$$\frac{d^3\Gamma}{dE_e dq^2 dq_0}$$
$$= \frac{G_F^2|V_{qb}|^2}{16\pi^3 M}\Big[W_1 q^2 + W_2(2E_e q_0 - 2E_e^2 - \frac{q^2}{2})$$
$$+W_3\frac{q^2}{M}(q_0 - 2E_e)\Big]\,. \qquad (7)$$

The structure functions W_4 and W_5 do not appear above because their contribution is proportional to the square of the electron mass and we ignore the lepton masses. In this general formalism the unknown hadronic structure resides in the functions W_a.

3 Light-cone dominance

It is well known that integrals like the one in (5) are dominated by distances where

$$0 \leq y^2 \leq \frac{1}{q^2}\,. \qquad (8)$$

For inclusive semileptonic B-meson decays (1), q^2 is time-like and varies in the physical range

$$0 \leq q^2 \leq (M - M_{X_{min}})^2\,. \qquad (9)$$

For extended regions of phase space the momentum transfer squared satisfies $q^2 \geq q^2_{ref}$ with $q^2_{ref} \simeq 1\,\text{GeV}^2$. In these regions we expect the dominant contribution to the integral in (5) to come from distances of the current commutator close to the light-cone. The commutator in this region is in fact singular leading to the dominant contribution

$$\langle B| \left[j_\mu(y), j_\nu^\dagger(0)\right] |B\rangle = 2(S_{\mu\alpha\nu\beta} - i\varepsilon_{\mu\alpha\nu\beta}) \left[\partial^\alpha \Delta_q(y)\right] \times \langle B|\bar{b}(0)\gamma^\beta(1-\gamma_5)b(y)|B\rangle \,, \quad (10)$$

where $S_{\mu\alpha\nu\beta} = g_{\mu\alpha}g_{\nu\beta} + g_{\mu\beta}g_{\nu\alpha} - g_{\mu\nu}g_{\alpha\beta}$ and $\Delta_q(y)$ is the Pauli-Jordan function for a free q-quark of mass m_q. The factor in the square bracket in (10) with the derivative of the Pauli-Jordan function has a singularity on the light-cone. The last factor with the reduced matrix element contains the long-distance contribution. The product of those two factors is Lorentz covariant and can be calculated in any Lorentz frame of reference.

The reduced matrix element has a simple Lorentz structure. It is in general a function of two scalars y^2 and $y \cdot P$ and can be expanded in powers of y^2:

$$\langle B|\bar{b}(0)\gamma^\beta(1-\gamma_5)b(y)|B\rangle = 4\pi P^\beta \sum_{n=0}^{\infty}(y^2)^n F_n(y\cdot P) \,. \quad (11)$$

We shall keep the first term of the series because the higher order terms are suppressed by powers of q^{-2}. This approximation is justified provided the coefficients are not very large. We can estimate the coefficients in quark models or the heavy quark effective theory which indicate that they satisfy

$$(y^2)^n F_n(y\cdot P) \approx e^{-im_b v\cdot y}(\Lambda^2_{QCD}/q^2)^n \,, \quad (12)$$

where v is the velocity of the initial B meson, defined by $v = P/M$. This behavior motivates the truncation of the series by keeping the first term with $n = 0$.

The Fourier transform of $F_0(y \cdot P)$ defines the quark distribution function

$$f(\xi) = \frac{1}{4\pi M^2}\int d(y\cdot P) e^{i\xi y\cdot P} \times \langle B|\bar{b}(0)\not{P}(1-\gamma_5)b(y)|B\rangle|_{y^2=0} \,. \quad (13)$$

We can use the inverse Fourier transform

$$F_0(y\cdot P) = \frac{1}{2\pi}\int d\xi e^{-i\xi y\cdot P} f(\xi) \quad (14)$$

and substitute F_0 in (11), (10) and (5), then carry out the y-integration in (5) and arrive at

$$W_{\mu\nu} = 4(S_{\mu\alpha\nu\beta} - i\varepsilon_{\mu\alpha\nu\beta})\int d\xi f(\xi)\varepsilon(\xi P_0 - q_0) \times \delta\left[(\xi P - q)^2 - m_q^2\right](\xi P - q)^\alpha P^\beta \,. \quad (15)$$

The components of the tensor $W_{\mu\nu}$ are expressed in terms of the distribution function. We have shown that the dominance of the light-cone makes possible the expression of the decay rate in terms of a quark distribution function defined in (13).

A special consequence of the decay kinematics is the occurrence of two roots in the argument of the δ-function in (15), namely

$$\xi_\pm = \frac{q\cdot P \pm \sqrt{(q\cdot P)^2 - M^2(q^2 - m_q^2)}}{M^2} \,. \quad (16)$$

We shall elaborate on this property below. The light-cone dominance ascribes the five hadronic structure functions to a single light-cone distribution function. The explicit relations are the following

$$W_1 = 2[f(\xi_+) + f(\xi_-)] \,, \quad (17)$$

$$W_2 = \frac{8}{\xi_+ - \xi_-}[\xi_+ f(\xi_+) - \xi_- f(\xi_-)] \,, \quad (18)$$

$$W_3 = -\frac{4}{\xi_+ - \xi_-}[f(\xi_+) - f(\xi_-)] \,, \quad (19)$$

$$W_4 = 0 \,, \quad (20)$$

$$W_5 = W_3 \,. \quad (21)$$

The structure functions are evaluated in two variables $\xi_\pm$. The second root, ξ_-, is a straightforward consequence of the analysis and corresponds to the creation of quark-antiquark pairs through the Z-diagram because the energy of the final quark is negative. The kinematic ranges for $\xi_\pm$ are

$$\frac{m_q}{M} \le \xi_+ \le 1 \,, \quad (22)$$

$$-\frac{m_q}{M} \le \xi_- \le 1 - \frac{2m_q}{M} \,. \quad (23)$$

In the light-cone and away from the resonance region $f(\xi_-)$ is relatively small. For $b \to c$ decays $\xi_- \lesssim 0.5$ where $f(\xi_-)$ is negligibly small. Scaling of the structure functions with the scaling variable ξ_+ holds when $f(\xi_-)$ is negligible [3].

The expression of the structure functions W_a in terms of a single distribution function, which depends on two values $\xi_\pm$ of the scaling variable, is a large simplification. Substituting the structure functions in (7) we arrive at

$$\frac{d^3\Gamma}{dE_e dq^2 dq_0} = \frac{G_F^2|V_{qb}|^2}{4\pi^3 M}\frac{q_0 - E_e}{\sqrt{\mathbf{q}^2 + m_q^2}} \times \left\{f(\xi_+)(2\xi_+ E_e M - q^2) - (\xi_+ \to \xi_-)\right\} \,. \quad (24)$$

The remaining unknown function is the reduced matrix element on the light-cone whose Fourier transform appears as the b-quark distribution function.

4 Properties of the distribution function

The distribution function obeys positivity and is zero for $\xi \le 0$ or $\xi \ge 1$ [3]. Three sum rules for the b-quark distribution function are known. The first one expresses the b quark number conservation [3]

$$\int_0^1 d\xi f(\xi) = 1 \,. \quad (25)$$

Performing the operator product expansion to reduce the bilocal operator to local ones and following [5–7] in order to expand the matrix element of the local operator in the HQET, two more sum rules were derived. They determine up to order $(\Lambda_{QCD}/m_b)^2$ the mean value μ and the variance σ^2 of the distribution function, which characterize the position of the maximum and its width, respectively:

$$\mu \equiv \int_0^1 d\xi \xi f(\xi) = \frac{m_b}{M}(1+E_b)\,, \tag{26}$$

$$\sigma^2 \equiv \int_0^1 d\xi (\xi-\mu)^2 f(\xi) = \frac{m_b^2}{M^2}\left(\frac{2K_b}{3} - E_b^2\right)\,, \tag{27}$$

where

$$G_b = \frac{1}{2M}\left\langle B \left| \bar{h}_v \frac{g G_{\alpha\beta}\sigma^{\alpha\beta}}{4m_b^2} h_v \right| B \right\rangle\,, \tag{28}$$

$$K_b = -\frac{1}{2M}\left\langle B \left| \bar{h}_v \frac{(iD)^2}{2m_b^2} h_v \right| B \right\rangle\,, \tag{29}$$

with $E_b = G_b + K_b$. The first matrix element G_b parametrizes the chromomagnetic energy arising from the b quark spin and is determined by the mass splitting between B^* and B mesons [5–7]. For the observed difference $M_{B^*} - M_B = 0.046$ GeV

$$m_b G_b = -\frac{3}{4}(M_{B^*} - M_B) = -0.034 \text{ GeV}\,. \tag{30}$$

The second matrix element K_b parametrizes the kinetic energy of the b quark in the B meson. It is determined with the help of QCD sum rules and carries a larger error, leading to the result [22]

$$2m_b^2 K_b = 0.5 \pm 0.2 \text{ GeV}^2\,. \tag{31}$$

Taking $m_b = 4.9 \pm 0.2$ GeV, the mean value and the variance of the distribution function are estimated to be

$$\mu = 0.93 \pm 0.04\,, \tag{32}$$

$$\sigma^2 = 0.006 \pm 0.002\,, \tag{33}$$

indicating that the distribution function is sharply peaked around its mean value, which is close to one. These results are consistent with the original expectations that the distribution function of a heavy quark peaks at a large value of its argument.

5 QCD radiative corrections

Special attention must be paid to the radiative corrections from the emission of gluons and the associated virtual diagrams. QCD radiative corrections to the electron energy spectra were studied in several articles [14–19], where they were calculated at the quark level. As already mentioned in the introduction, in the application of radiative corrections at the hadron level we encounter two problems: the first is to change the quark phase space to the physical one and the second is the treatment of the logarithmic singularities to order α_s, which appear at the quark-level endpoints $E_e = \frac{m_b}{2}(1 - \frac{m_q^2}{m_b^2})$.

These problems may be solved by taking into account the bound state effect. In the decay of a B-meson, the perturbative QCD correction will be modified by the bound state effects, since QCD confinement implies that free quarks are not asymptotic states of the theory. The bound state effect is described by the b-quark distribution function given in (13), which is the probability of finding a b quark with momentum ξP inside the B-meson. The substitution of the b quark momentum p_b by ξP introduces the hadronic phase space. Furthermore, the radiative corrections obtained perturbatively must be convoluted with the distribution function. The final contribution for the radiative corrections is given by

$$\frac{d\Gamma_{rad}}{dE_e} = \int_{\frac{E_e + \sqrt{E_e^2 + m_q^2}}{M}}^1 d\xi\, f(\xi) \left(\frac{d\Gamma_{rad}^b}{dE_e}\right)_{p_b = \xi P}\,, \tag{34}$$

where the quark-level $O(\alpha_s)$ perturbative QCD correction $d\Gamma_{rad}^b/dE_e$ was computed analytically in [17,18]. In this way the endpoints of the perturbative spectra are extented from the quark level to the hadron level and the logarithmic singularities are eliminated. As we shall see, the interplay between perturbative and nonperturbative QCD effects is important, especially for the shape of the $b \to u$ electron energy spectrum near the endpoint.

We could give at this point formulas for the radiative corrections at the quark level, but since they are available in two articles [17,18] we refer to them. The interested reader may consult these articles and use their formulas for $d\Gamma_{rad}^b/dE_e$ which occurs in (34). An important property of (34) is that the integral over ξ eliminates the logarithmic singularities.

In order to calculate the decay spectra we need a distribution function $f(\xi)$ consistent with the properties of Sect. 4. We propose the Ansatz

$$f(\xi) = N \frac{\xi(1-\xi)}{(\xi - a)^2 + b^2}\theta(\xi)\theta(1-\xi)\,, \tag{35}$$

where N is the normalization constant and a and b two parameters. For $a = m_b/M$ and $b = 0$, this distribution function reduces to a delta function, $\delta(\xi - m_b/M)$, and thus reproduces the free-quark decay model. In addition, the constraints (32) and (33), stemming from the HQET, limit the two constants a and b. Other forms of the distribution function have been proposed in [23,24].

We use (24), (34) and (35) to compute the electron energy spectra for $b \to c$ and $b \to u$ decays. The calculation is done using (24) by integrating first over q_0 and then over q^2 with the integration limits

$$E_e + \frac{q^2}{4E_e} \le q_0 \le \frac{q^2 + M^2 - M_{X_{min}}^2}{2M}\,, \tag{36}$$

$$0 \le q^2 \le 2E_e\left(M - \frac{M_{X_{min}}^2}{M - 2E_e}\right)\,. \tag{37}$$

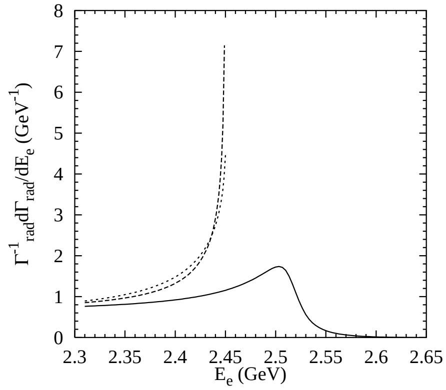

Fig. 1. Comparison of the radiative correction to the $b \to u$ electron energy spectrum in the endpoint region as calculated in this paper (*solid line*) with the quark-level results of [18] without (*long-dashed line*) and with (*short-dashed line*) the Sudakov exponentiation for $\alpha_s = 0.25, m_b = 4.9$ GeV, $m_u = 0$, $a = 0.953$ and $b = 0.00560$

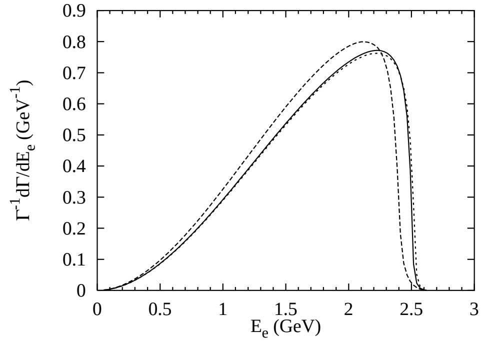

Fig. 2. The shape of the electron energy spectrum from the $b \to u$ inclusive semileptonic B meson decay in the rest frame of the B meson for various values of parameters: (1) $m_u = 0$, $\mu = 0.93$, $\sigma^2 = 0.006$ ($a = 0.953, b = 0.00560$) (*solid line*); (2) $m_u = 0$, $\mu = 0.89$, $\sigma^2 = 0.006$ ($a = 0.913, b = 0.00992$) (*long-dashed line*); (3) $m_u = 0$, $\mu = 0.93$, $\sigma^2 = 0.008$ ($a = 0.960, b = 0.00679$) (*short-dashed line*). The strong coupling constant is fixed to be $\alpha_s = 0.25$

For practical calculations we take $M_{X_{min}} = m_q$ on the assumption of quark-hadron duality.

The parameters which enter in the calculation are the final quark mass m_q, the parameters a and b (or the equivalent quantities: the mean value μ and the variance σ^2) of the distribution function and the strong coupling constant α_s. An important feature is the appearance in the decay rates of the physical B-meson mass instead of the b quark mass.

The necessity of taking into account the interplay between perturbative and nonperturbative QCD effects on both $b \to c$ and $b \to u$ spectra is discussed above. Here we illustrate in Fig. 1 that this interplay is important especially in the endpoint region of the $b \to u$ spectrum. The radiative correction calculated with the help of (34) is a smooth function of the electron energy up to the physical endpoint (solid curve). The other two curves show the quark-level perturbative correction without and with the Sudakov exponentiation [16], respectively. Radiative corrections without the Sudakov exponentiation run off to infinity with increasing energy as expected. The Sudakov exponentiation eliminates the singularity and gives a decay rate finite up to the quark-level endpoint $E_e = \frac{m_b}{2}$. Beyond this value the correction is zero. For our case, the radiative correction, shown in Fig. 1, remains finite all the way up to the physical endpoint $E_e = \frac{M}{2}$.

The property that the averaging over a variable of the initial quark renders the radiative corrections finite is general. For example, the authors in [12] introduced a smearing over the b-quark momentum, which renders the perturbatively calculated spectra finite. Similarly, the averaging over the momentum distribution of the spectator in the ACCMM model [16] makes the radiative corrections finite. The authors in [25] computed the hadron energy spectrum including radiative corrections. For the ACCMM model they included the averaging over the Fermi motion, which makes the perturbative term finite.

6 Electron energy spectra

Having at our disposal a coherent treatment of perturbative and nonperturbative QCD effects, we study the sensitivity of the shape of the spectrum to various parameters. As discussed in the previous section, we use (24), (34) and (35) to compute the spectra. More precisely, we integrate (24) over q_0 and q^2 and then add the QCD radiative correction from (34) to obtain the radiatively corrected electron spectrum.

The $b \to u$ spectrum is shown in Fig. 2 as a function of μ and σ^2. It is evident that the spectrum is much more sensitive to the mean value μ of the distribution function than its variance σ^2. The shape of the spectrum is insensitive to the value of the mass of the final quark m_u. The effect of the radiative corrections on the spectrum is shown in Fig. 3 where we have chosen two values of $\alpha_s = 0.25$ (solid curve) and $\alpha_s = 0$ (dashed curve). The effect of the radiative correction is moderate.

The spectrum near the endpoint is important for the determination of $|V_{ub}|$. We study the sensitivity of the endpoint spectrum to two different distribution functions. In addition to the distribution in (35) we use the Ansatz from [23], for which we fix the parameters to satisfy the central values of the sum rules in (32) and (33). Then we calculate the $b \to u$ spectra shown in Fig. 4. We note that the two curves are close to each other. The corresponding partial decay width to the endpoint region 2.31 GeV$\leq E_e \leq$ 2.64 GeV is calculated to be $10.7|V_{ub}|^2\text{ps}^{-1}$ using (35) and $11.5|V_{ub}|^2\text{ps}^{-1}$ using the Ansatz from [23], respectively. These suggest that the determination of $|V_{ub}|$ from the endpoint spectrum does not depend strongly on the Ansatz for the distribution function.

We study next the dependence of the shape of the electron energy spectrum for the $b \to c$ decay on various parameters. In addition to the previous parameters, the mass of the charm quark plays now a role. We show in Fig. 5 the electron spectrum as a function of m_c, μ and σ^2. The

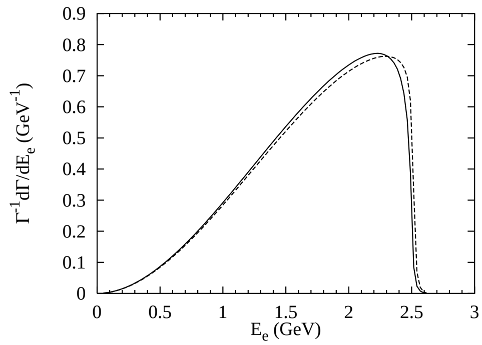

Fig. 3. The shape of the electron energy spectrum from the $b \to u$ inclusive semileptonic B meson decay in the rest frame of the B meson for $m_u = 0$, $\mu = 0.93$, $\sigma^2 = 0.006$ ($a = 0.953, b = 0.00560$), $\alpha_s = 0.25$ (*solid line*) and $\alpha_s = 0$ (*dashed line*)

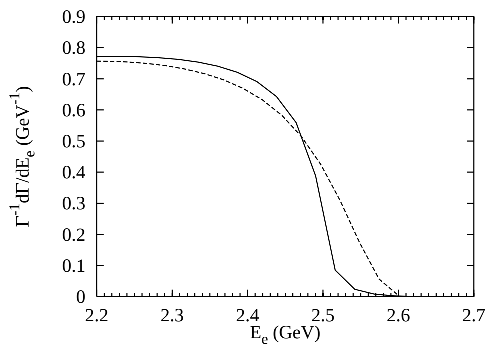

Fig. 4. The shape of the $b \to u$ endpoint spectrum in the rest frame of the B meson using (35) (*solid line*) and the Ansatz from [23] (*dashed line*) for $\alpha_s = 0.25, m_u = 0, \mu = 0.93$ and $\sigma^2 = 0.006$

shape of the spectrum is a sensitive function of the mass of the charm quark m_c and of the mean value μ. It is rather insensitive to the variance σ^2. In Fig. 6 we show the electron spectrum with and without radiative corrections. It is evident that the $b \to c$ spectrum is insensitive to the value of α_s.

With the parameters determined so far we can calculate the $b \to c$ spectrum and compare it with the recent experimental data from the CLEO collaboration [26]. We present our result in Fig. 7, where the theoretical curve has been boosted to the rest frame of the $\Upsilon(4S)$ resonance. The curve for the central values of the sum rules in (32) and (33) passes to the right of the experimental points. For this reason we searched for values of a and b consistent with the sum rules which reproduce the data. The result is shown in Fig. 7 for $a = 0.931$ and $b = 0.0118$ corresponding to $\mu = 0.90$ and $\sigma^2 = 0.008$.

The above analyses indicate the sensitivity of the spectral shape to various parameters and imply that a detailed fit[1] to the measured spectrum can impose strong constraints on the mean value of the distribution function and the mass of the charm quark. This procedure will re-

[1] Such a fit should also account for detector resolution and bremsstrahlung

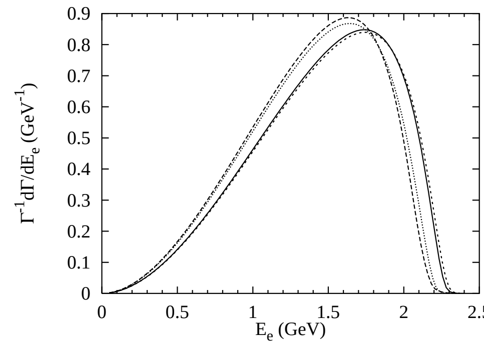

Fig. 5. The shape of the electron energy spectrum from the $b \to c$ inclusive semileptonic B meson decay in the rest frame of the B meson for various values of parameters: (1) $m_c = 1.5$ GeV, $\mu = 0.93$, $\sigma^2 = 0.006$ ($a = 0.953, b = 0.00560$) (*solid line*); (2) $m_c = 1.5$ GeV, $\mu = 0.89$, $\sigma^2 = 0.006$ ($a = 0.913, b = 0.00992$) (*long-dashed line*); (3) $m_c = 1.5$ GeV, $\mu = 0.93$, $\sigma^2 = 0.008$ ($a = 0.960, b = 0.00679$) (*short-dashed line*); (4) $m_c = 1.7$ GeV, $\mu = 0.93$, $\sigma^2 = 0.006$ ($a = 0.953, b = 0.00560$) (*dotted line*). The strong coupling constant is fixed to be $\alpha_s = 0.25$

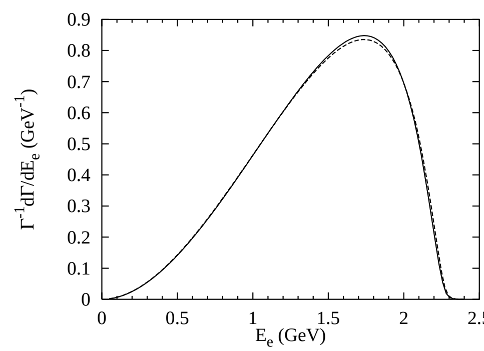

Fig. 6. The shape of the electron energy spectrum from the $b \to c$ inclusive semileptonic B meson decay in the rest frame of the B meson for $m_c = 1.5$ GeV, $\mu = 0.93$, $\sigma^2 = 0.006$ ($a = 0.953, b = 0.00560$), $\alpha_s = 0.25$ (*solid line*) and $\alpha_s = 0$ (*dashed line*)

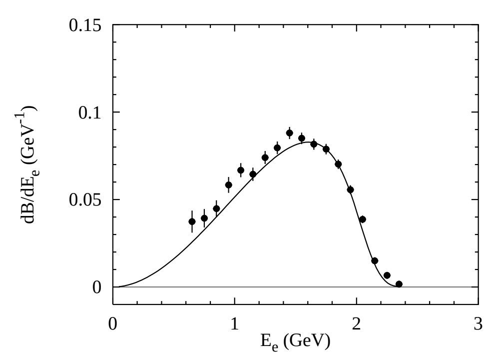

Fig. 7. The predicted electron energy spectrum compared with the CLEO data. The theoretical calculation uses $m_c = 1.61$ GeV, $a = 0.931$, $b = 0.0118$, $\alpha_s = 0.25$ and $\beta = 0.061$ for the velocity of the B meson. The spectrum is normalized to the B-meson semileptonic branching fraction

duce the theoretical uncertainty in the calculation of the semileptonic decay width of the B-meson [27] and improve the accuracy of the predictions for the $b \to u$ spectrum. Precise determinations of $|V_{cb}|$ and $|V_{ub}|$ may be gained from inclusive semileptonic B-meson decays. Finally, the same tensor structure appears in the decay $B \to J/\psi + X$ [28] and a universal fit of both processes would be of interest. Dedicated studies of the inclusive B decays will also offer more insight into the internal structure of hadrons.

Acknowledgements. We would like to thank R. Poling and R. Wang for kindly providing us with their data on inclusive B decays and P. Soldan for reading the paper. The financial support of the Bundesministerium für Bildung und Forschung under contract No. 056DO93P(6) is gratefully acknowledged.

References

1. A. Bareiss and E.A. Paschos, Nucl. Phys. **B 327** (1989) 353;
   A. Bareiss, Z. Phys. **C 53** (1992) 311
2. C.H. Jin, W.F. Palmer, and E.A. Paschos, Phys. Lett. **B 329** (1994) 364
3. C.H. Jin and E.A. Paschos, in: Proceedings of the International Symposium on Heavy Flavor and Electroweak Theory, Beijing, China, 1995, edited by C.H. Chang and C.S. Huang (World Scientific, Singapore, 1996), p.132; DO-TH 95/07, hep-ph/9504375
4. J. Chay, H. Georgi, and B. Grinstein, Phys. Lett. **B 247** (1990) 399
5. I.I. Bigi, N.G. Uraltsev, and A.I. Vainshtein, Phys. Lett. **B 293** (1992) 430 [E: 297 (1993) 477];
   I.I. Bigi, M.A. Shifman, N.G. Uraltsev, and A.I. Vainshtein, Phys. Rev. Lett. 71 (1993) 496
6. A.V. Manohar and M.B. Wise, Phys. Rev. **D 49** (1994) 1310
7. B. Blok, L. Koyrakh, M.A. Shifman, and A.I. Vainshtein, Phys. Rev. **D 49** (1994) 3356 [E: 50 (1994) 3572]
8. M. Luke and M.J. Savage, Phys. Lett. **B 321** (1994) 88;
   A.F. Falk, M. Luke, and M.J. Savage, Phys. Rev. **D 49** (1994) 3367
9. T. Mannel, Nucl. Phys. **B 413** (1994) 396
10. A.F. Falk, Z. Ligeti, M. Neubert, and Y. Nir, Phys. Lett. **B 326** (1994) 145
11. M. Neubert, Phys. Rev. **D 49** (1994) 3392 and 4623;
    T. Mannel and M. Neubert, Phys. Rev. **D 50** (1994) 2037
12. I.I. Bigi, M.A. Shifman, N.G. Uraltsev, and A.I. Vainshtein, Int. J. Mod. Phys. **A 9** (1994) 2467
13. For the status of this field, see a recent review: M. Neubert, CERN-TH/97-24, hep-ph/9702375, to appear in: Heavy Flavours (Second Edition), edited by A.J. Buras and M. Lindner (World Scientific, Singapore)
14. A. Ali and E. Pietarinen, Nucl. Phys. **B 154** (1979) 519
15. N. Cabibbo, G. Corbo, and L. Maiani, Nucl. Phys. **B 155** (1979) 93
16. G. Altarelli, N. Cabibbo, G. Corbo, L. Maiani, and G. Martinelli, Nucl. Phys. **B 208** (1982) 365
17. G. Corbo, Nucl. Phys. **B 212** (1983) 99
18. M. Jezabek and J.H. Kühn, Nucl. Phys. **B 320** (1989) 20
19. M. Gremm and I. Stewart, Phys. Rev. **D 55** (1997) 1226
20. T. Kinoshita, J. Math. Phys. **3** (1962) 650;
    T.D. Lee and M. Nauenberg, Phys. Rev. **B 133** (1964) 1549
21. E.C. Poggio and H.R. Quinn, Phys. Rev. **D 14** (1976) 578;
    G. Sterman, Phys. Rev. **D 14** (1976) 2123
22. P. Ball and V. Braun, Phys. Rev. **D 49** (1994) 2472
23. K.Y. Lee and J.K. Kim, Phys. Lett. **B 377** (1996) 153
24. C. Peterson, D. Schlatter, J. Schmitt, and P.M. Zerwas, Phys. Rev. **D 27** (1983) 105
25. C. Greub and S.-J. Rey, SLAC-PUB-7245, hep-ph/9608247
26. CLEO Collaboration, B. Barish et al., Phys. Rev. Lett. 76 (1996) 1570
27. C.H. Jin, LMU 08/96, hep-ph/9610543, to appear in Phys. Rev. **D**
28. W.F. Palmer, E.A. Paschos, and P.H. Soldan, DO-TH 97/04, DOE/ER/01545-709, OHSTPY-HEP-97-003, hep-ph/9701328